WEP Warwick Evans Publishing

International Journal of Mechanical and Electrical Engineering

ISSN: 3005-9615 (Print), ISSN: 3005-7132 (Online) | Volume 8, Number 1, Year 2026
DOI: https://doi.org/10.62051/ijmee.v8n1.05
Journal homepage: https://wepub.org/index.php/IJMEE/index

Research on Optimization of Spiral Bevel Gear Milling Parameters Based on the Levenberg-Marquardt Method

Zeyu Fang

School of Mechanical Engineering, Tianjin University of Technology and Education, Tianjin, 300350, China

ABSTRACT

Based on the milling principle of spiral bevel gears, the structure of the spiral bevel gear milling machine and the motion relationships among its axes were analyzed, and a generating machining motion model for spiral bevel gears was established. By integrating the parameters of the milling cutter head with the generating machining motion model, a tooth surface model enveloped by the cutter head was developed. An analysis was conducted on the influence of six milling process parameters—such as angular tool position, radial tool position, and workpiece blank installation angle—on tooth surface deviation. Building on this foundation, an optimization model aimed at minimizing tooth surface deviation was constructed. The L-M algorithm was then employed to iteratively optimize the machining parameters with the goal of reducing the theoretical machining error as much as possible.

KEYWORDS

Spiral Bevel Gears; Levenberg-Marquardt Method; Optimization of Milling Parameters.

1. INTRODUCTION

In production, due to errors in the feedback of pulse signals from the CNC system servo motors, adjustments such as the tool position vector, horizontal work offset, vertical work offset, and bed position—driven by linear motion axes—may experience errors of ±0.02 mm. Meanwhile, adjustments like the tool polar angle and workpiece installation angle, driven by rotational motion axes, may incur errors of ±2'. As a result, deviations arise between the actual machined tooth surface and the theoretical tooth surface [1]. To minimize the theoretical machining error in the tooth profile of spiral bevel gears, it is essential to optimize the milling process parameters.

Regarding the issue of tooth surface error correction for spiral bevel gears, numerous scholars have conducted systematic research. Based on the mapping relationship between machine tool processing parameters and tooth surface errors, Li Qiming [2]proposed a corresponding method for tooth surface error correction. Su Jinzhan and Fang Zongde [3]enhanced the meshing stability of spiral bevel gears by introducing a tooth surface modification strategy with low sensitivity. They established a mathematical relationship between tooth profile errors and an error sensitivity coefficient matrix, constructed a tooth profile error correction model, and employed the least squares method to optimize the solution of this transcendental equation system, thereby obtaining the correction values for machine tool adjustment parameters. Cai Xiangwei, Fang Zongde, et al. [4], taking spiral bevel gears as the research subject, built an optimization model for approximating the theoretical tooth surface to the target tooth surface, explored implementation approaches for relevant algorithms, and laid a theoretical foundation for tooth surface error correction technology. Wang Xiaochun, Wang Jun, et al. [5], based on the theoretical tooth surface model of Gleason spiral bevel gears, used a difference

surface to characterize the deviation between the actual and theoretical tooth surfaces, and proposed a correction method for machine tool adjustment parameters, which was proven to significantly improve tooth surface accuracy. Chen Shuhan and Yan Hongzhi[6], addressing the characteristics of spiral bevel gear tooth surface deviation identification and the limitations of the least squares method in solving such problems, proposed a solution strategy combining the Truncated Singular Value Decomposition (TSVD) method with the L-curve method, and verified the accuracy of this approach. Nie Shaowu et al[7]. established a mathematical correction model between tooth surface deviations and machine tool processing parameters, and inversely calculated the machine tool processing parameters for modified tooth surfaces based on the least squares method. Lin [8]studied a linear regression method for reducing tooth surface deviations, established a mathematical model for hypoid gears, achieved minimization of tooth surface deviations using a sensitivity coefficient matrix and linear regression method, and employed the Singular Value Decomposition (SVD) method to solve this minimization problem, providing a reference for improving traditional processes.

In summary, the functional relationship between tooth profile deviations of spiral bevel gears and machine tool adjustment parameters exhibits strong nonlinear characteristics. When using the linear least squares method for solution, results often become unstable due to ill-conditioned or singular Jacobian matrices. To improve solution stability, employing a nonlinear least squares method to address this problem can be considered.

2. TOOTH SURFACE MODELING OF SPIRAL BEVEL GEARS

2.1. Kinematic Model for the Generating Machining of Spiral Bevel Gears

According to the machining principle of spiral bevel gears, the structure of the spiral bevel gear milling machine and the kinematic relationships among its axes are analyzed to construct a generating machining motion model for spiral bevel gears. The milling process of spiral bevel gears is accomplished through the coordinated movement of six axes: three translational axes—including the X-axis moving horizontally, the Y-axis moving vertically, and the Z-axis sliding with the workpiece carriage—and three rotational axes—including the workpiece rotation A-axis, the workpiece carriage rotation B-axis, and the tool rotation C-axis . By simultaneously coordinating the motions of these six axes, the relative tool-workpiece motion relationship in the generating process can be accurately simulated. This provides a basis for deriving the tooth surface equation of the gear and solving for the conjugate surface. A schematic diagram of the machine tool structure is shown in Figure 1.

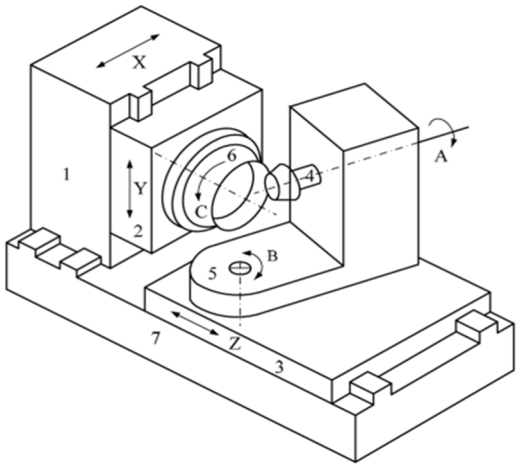

Figure 1. The generative machining motion model of spiral bevel gear milling machines

Based on the structure and kinematic relationships of the spiral bevel gear milling machine, the machining coordinate system for the spiral bevel gear milling machine is established, as shown in Figure 2. In the figure, $S_2\{O_2;X_2,Y_2,Z_2\}$ is the workpiece coordinate system, $S_m\{O_m;X_m,Y_m,Z_m\}$is the

machine tool coordinate system, $S_C\{O_C; X_C, Y_C, Z_C\}$ is the generating gear coordinate system, $S_3\{O_3; X_3, Y_3, Z_3\}$ is the cutter head coordinate system, while $S_W\{O_W; X_W, Y_W, Z_W\}$, $S_t\{O_t; X_t, Y_t, Z_t\}$, and $S_n\{O_n; X_n, Y_n, Z_n\}$ are auxiliary coordinate systems. Here, $\boldsymbol{q}$ denotes the angular tool position, $\boldsymbol{S}$ the radial tool position, $\boldsymbol{X}_b$ the sliding base position, $\boldsymbol{\delta}_m$ the workpiece blank installation angle, $\boldsymbol{X}_p$ the axial work offset, and $\boldsymbol{E}$ the vertical work offset.

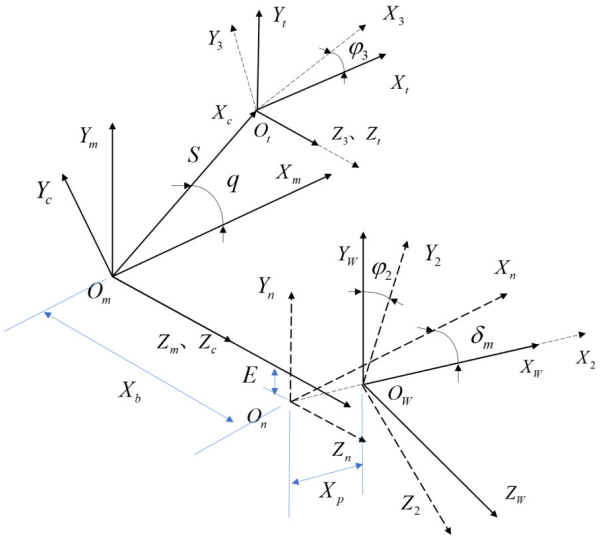

Figure 2. Machining Coordinate System

The coordinate transformation matrices between the respective coordinate systems are given by Eqs. (1)–(3):

$$M_{w1}=\begin{bmatrix}1 & 0 & 0 & 0\\ 0 & \cos\varphi_1 & -\sin\varphi_1 & 0\\ 0 & \sin\varphi_1 & \cos\varphi_1 & 0\\ 0 & 0 & 0 & 1\end{bmatrix} \quad M_{nw}=\begin{bmatrix}\cos\delta_M & 0 & \sin\delta_M & -X_p\\ 0 & 1 & 0 & 0\\ -\sin\delta_M & 0 & \cos\delta_M & 0\\ 0 & 0 & 0 & 1\end{bmatrix} \tag{1}$$

$$M_{mn}=\begin{bmatrix}1 & 0 & 0 & 0\\ 0 & 1 & 0 & -E\\ 0 & 0 & 1 & -X_B\\ 0 & 0 & 0 & 1\end{bmatrix} \quad M_{cm}=\begin{bmatrix}\cos q & -\sin q & 0 & 0\\ \sin q & \cos q & 0 & 0\\ 0 & 0 & 1 & 0\\ 0 & 0 & 0 & 1\end{bmatrix} \tag{2}$$

$$M_{tc}=\begin{bmatrix}1 & 0 & 0 & S\\ 0 & 1 & 0 & 0\\ 0 & 0 & 1 & 0\\ 0 & 0 & 0 & 1\end{bmatrix} \quad M_{2t}=\begin{bmatrix}\cos\varphi_2 & -\sin\varphi_2 & 0 & 0\\ \sin\varphi_2 & \cos\varphi_2 & 0 & 0\\ 0 & 0 & 1 & 0\\ 0 & 0 & 0 & 1\end{bmatrix} \tag{3}$$

Let the position of the cutter head center in the machining coordinate system be represented by the vector $\boldsymbol{n}_t$=[0; 0; 0; 1], and its unit orientation vector be $\boldsymbol{N}_t$=[0; 0; 1; 0].

Through coordinate transformation, the position of the cutter head center in the workpiece coordinate system S_2 can be represented by the vector $\boldsymbol{n}_2$:

$$\boldsymbol{n}_2 = M_{2w}M_{wn}M_{nm}M_{mc}M_{ct}M_{t3}\boldsymbol{n}_t \tag{4}$$

The unit orientation vector of the cutter head center in the workpiece coordinate system S_2 is $\boldsymbol{N}_2$:

$$\boldsymbol{N}_2 = M_{1w}M_{wn}M_{nm}M_{mc}M_{ct}M_{t3}\boldsymbol{N}_t \tag{5}$$

To obtain the position of each motion axis at every instant, the position vector of the cutter center needs to be transformed from the workpiece coordinate system to the CNC machine tool coordinate system. Let the swing angle of the workpiece carriage spindle on the CNC machine tool be B, and the rotation angle of the workpiece rotation axis, which is fixed and synchronized with the workpiece carriage, be A. The CNC machine tool coordinate system is denoted as $S_A\{O_A; X_A, Y_A, Z_A\}$, the workpiece coordinate system as $S_B\{O_B; X_B, Y_B, Z_B\}$, and the coordinate system fixed to the workpiece as $S_C\{O_C; X_C, Y_C, Z_C\}$. The transformation matrices between these coordinate systems are:

$$M_{AB} = \begin{bmatrix} \cos B & 0 & \sin B & 0 \\ 0 & 1 & 0 & 0 \\ -\sin B & 0 & \cos B & 0 \\ 0 & 0 & 0 & 1 \end{bmatrix} \tag{6}$$

$$M_{BC} = \begin{bmatrix} 1 & 0 & 0 & 0 \\ 0 & \cos A & -\sin A & 0 \\ 0 & \sin A & \cos A & 0 \\ 0 & 0 & 0 & 1 \end{bmatrix} \tag{7}$$

In the CNC coordinate system, the axis of the cutter head is always perpendicular to the machine's X-O-Y plane. Therefore, the unit orientation vector of the cutter head center in the CNC coordinate system is $\boldsymbol{N}_A$=[0; 0; 1; 0]. Let the unit orientation vector of the cutter head center in the workpiece coordinate system S_2 be $\boldsymbol{N}_2$=[N_x; N_y; N_z; 0]. Then,

$$\boldsymbol{N}_A = M_{AB} M_{BC} \boldsymbol{N}_2 \tag{8}$$

By combining Equations (5) - (8), the expressions for the two rotational axes A and B in the CNC coordinate system can be obtained as shown in Equation (2.16), where the swing angle B ranges from 0° to 90°.

$$\begin{cases} A = \arctan(-N_y / N_z) \\ B = \arctan(-N_x / \sqrt{N_y^2 + N_z^2}) \end{cases} \tag{9}$$

Let the position vector of the cutter head center in the CNC coordinate system be $\boldsymbol{n}_A$=[n_x; n_y; n_z; 0]. Then,

$$\boldsymbol{n}_A = M_{AB} M_{BC} \boldsymbol{n}_1 \tag{10}$$

By combining Equations (4), (6), (7), and (10), the values for the three translational axes X, Y, and Z of the CNC machine tool can be obtained. These are the three components of the position vector $\boldsymbol{n}_A$ of the cutter head center in the CNC coordinate system, respectively.

$$\begin{cases} X = n_x \\ Y = n_y \\ Z = n_z \end{cases} \tag{11}$$

Equation (11) determines the position of each motion axis of the machine tool at every generating position, i.e., the corresponding cutter location point. Based on these cutter location points, the target tooth surface can be completely machined. Thus, the positions of the five coordinate axes (X, Y, Z, A, B) of the CNC machine tool at any moment during the tooth surface generation process are determined.

Based on the above analysis, the motion parameters of the corresponding servo axes at each generating position—i.e., the discrete cutter location data—can be obtained. This set of cutter location points constitutes the necessary tool path for machining the complete tooth surface. Furthermore, given process parameters such as the angular tool position q, workpiece blank installation angle δ_m, and roll ratio, along with machine adjustment parameters like vertical work offset and sliding base position, the positions of the five coordinate axes (X, Y, Z, A, B) of the CNC machine tool at any moment during the tooth surface generation process can be calculated using the kinematic model.

2.2. Tool Swept Trajectory Model

In the previous section, an analysis was conducted on the structure of the spiral bevel gear milling machine and the kinematic relationships among its axes, and a generating machining motion model for spiral bevel gears was established. During the generation machining of spiral bevel gears, the cradle angle continuously changes, and the spatial position of the milling cutter head also varies accordingly. The tooth surface is enveloped by the swept trajectory formed by the continuous motion of the cutter's cutting edge. The tooth surface formed by the envelope of the cutting edge trajectory is referred to as the cutting edge swept surface, and the set of such surfaces formed by multiple cuts is called the cutting edge swept surface cluster. To accomplish tooth surface modeling, it is necessary to first establish a mathematical model of the cutting edge, which is then substituted into the generating machining motion model to derive the swept trajectory of the cutting edge—that is, the mathematical model of the cutting edge swept surface.

Figure 3 shows the cross-sectional view of the cutting blade. Here, L_C represents the blade offset, l denotes the cutting edge length, r_o is the nose radius of the tool tip, α_i is the inner cutting edge pressure angle, α_o is the outer cutting edge pressure angle, and the rotation angle of the milling cutter head around the z-axis (i.e., the tool rotation axis) is defined as θ.

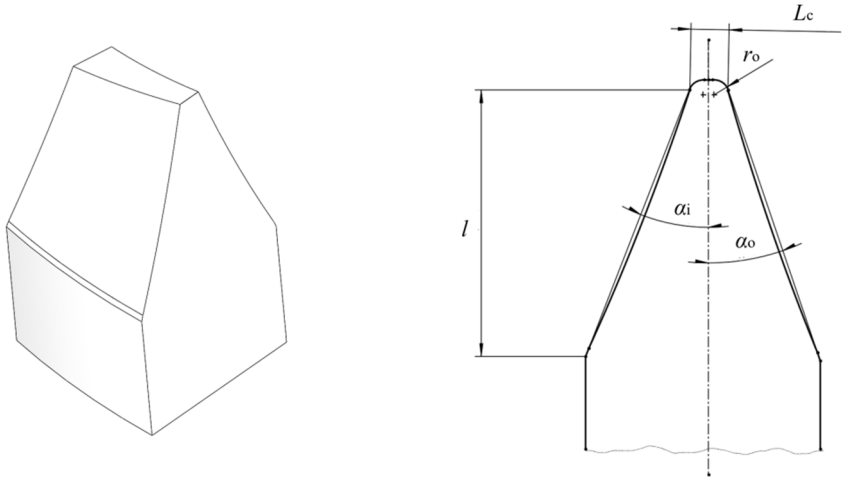

(a) 3D Model (b) Cross-sectional View

Figure 3. Cutting Blade

The cutting edge profile curve can be expressed as an equation in terms of the cutting edge length l, and thus the cutter head can be represented by an equation in terms of both l and θ:

$$\begin{cases} x = x(l,\theta) \\ y = y(l,\theta) \\ z = z(l,\theta) \end{cases} \tag{12}$$

Equations (1)-(3) represent the transformation matrices for mapping the cutter head from the tool coordinate system to the workpiece coordinate system during the generating machining process. The

cutting edge swept surface is obtained by discretizing the continuous generating process of the cutting edge into n segments. Consequently, the equation for the cutting edge swept surface can be expressed in terms of the parameters n, l, and θ.

$$\begin{cases} x\{n\} = x\{n\}(l,\theta) \\ y\{n\} = y\{n\}(l,\theta) \\ z\{n\} = z\{n\}(l,\theta) \end{cases} \tag{13}$$

By substituting a set of gear pair geometric parameters, the mathematical model of the workpiece gear blank is established. The basic parameters of the milling cutter head are then substituted into Equation (12), which defines the designed curved cutting edge. Next, using Equation (13), the continuous generating process of the cutter head is discretized into n segments, thereby obtaining the cutting edge swept surface model for the designed curved edge. Through programming in MATLAB software, the swept surface and the workpiece blank model are plotted, as shown in Figure 4. In the figure, the yellow section represents the outer conical surface of the workpiece gear blank, while the green and red sections represent the inner and outer cutting edge swept surface clusters, respectively. The inner and outer swept surface clusters collectively cut out a single tooth slot on the workpiece. Multiple sets of these inner and outer swept surface clusters (the number of sets depends on the number of teeth on the workpiece) are used to machine all tooth profiles.

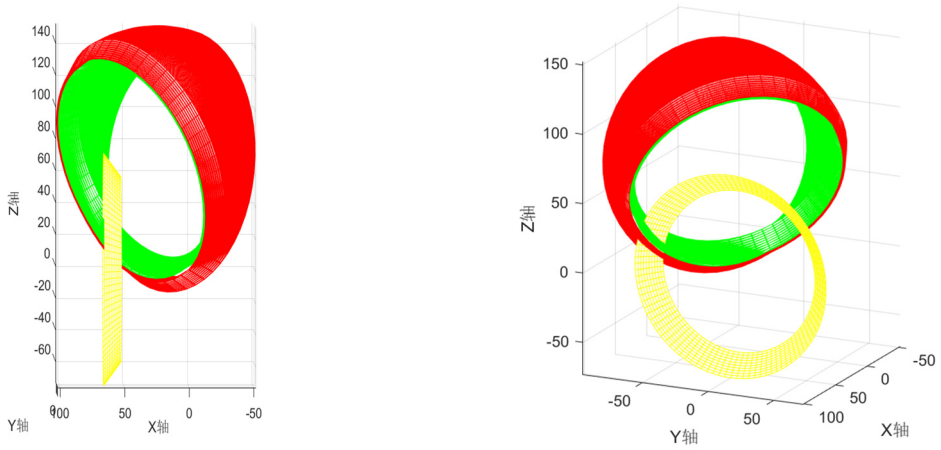

Figure 4. Tool Swept Trajectory

3. OPTIMIZATION OF MILLING PARAMETERS

In order to minimize the theoretical machining error of the spiral bevel gear tooth profile as much as possible, it is necessary to optimize the milling process parameters. The principle of the generating process for spiral bevel gear milling is illustrated in Figure 1. Key machine tool adjustment parameters, such as the angular tool position, radial tool position, workpiece blank installation angle, axial work offset, sliding base position, and vertical work offset, are not only critical for machine setup but also closely related to cutter design. These parameters can be taken as the optimization targets (design variables).

3.1. Analysis of the Influence of Milling Process Parameters on Tooth Surface Deviation

As discussed earlier, both the cutting edge swept surface equation and the tooth surface equation can be expressed as functions of parameters such as the angular tool position q and the workpiece blank installation angle δ_m. The tooth surface obtained above is taken as the theoretical tooth surface, while

the tooth surface containing the aforementioned parameter variables is regarded as the error tooth surface. Based on the established tooth surface equation, tooth surface discretization techniques can be employed to calculate and evaluate the deviation between the theoretical tooth surface and the actual error tooth surface. Typically, the discretized tooth surface is represented as a 9×5 point grid, with 9 columns along the tooth length direction and 5 rows along the tooth height direction, resulting in a total of 45 discrete points. By comparing the positions of the discrete points on the theoretical tooth surface with the corresponding points on the error tooth surface, the deviation value at each point can be obtained.

Various design variables are introduced into the milling process motion model, and their values can be obtained using the Quasi-Monte Carlo sampling method. This method generates samples based on deterministic low-discrepancy sequences (such as Halton sequences or Sobol sequences). Compared to the classical Monte Carlo method, which relies on pseudo-random number generators, the Quasi-Monte Carlo method offers better spatial uniformity and faster convergence for the same sample size, making it more suitable for analyzing systems with coupled multi-parameter variables.

After introducing the variables, the transformation matrices in the milling process motion model can be expressed as follows:

$$M_{nw}' = \begin{bmatrix} \cos(\Delta\delta_M) & 0 & \sin(\Delta\delta_M) & -\Delta X_p \\ 0 & 1 & 0 & 0 \\ -\sin(\Delta\delta_M) & 0 & \cos(\Delta\delta_M) & 0 \\ 0 & 0 & 0 & 1 \end{bmatrix} \tag{14}$$

$$M_{mn}' = \begin{bmatrix} 1 & 0 & 0 & 0 \\ 0 & 1 & 0 & -\Delta E \\ 0 & 0 & 1 & -\Delta X_B \\ 0 & 0 & 0 & 1 \end{bmatrix} \tag{15}$$

$$M_{cm}' = \begin{bmatrix} \cos(\Delta q) & -\sin(\Delta q) & 0 & 0 \\ \sin(\Delta q) & \cos(\Delta q) & 0 & 0 \\ 0 & 0 & 1 & 0 \\ 0 & 0 & 0 & 1 \end{bmatrix} \tag{16}$$

$$M_{tc}' = \begin{bmatrix} 1 & 0 & 0 & \Delta S \\ 0 & 1 & 0 & 0 \\ 0 & 0 & 1 & 0 \\ 0 & 0 & 0 & 1 \end{bmatrix} \tag{17}$$

By substituting Equations (14) to (17) into the generating machining motion model, the tooth surface model incorporating the design variables is obtained. Consequently, the tooth surface equation can be expressed as:

$$\boldsymbol{r} = \boldsymbol{r}(\Delta S, \Delta q, \Delta X_B, \Delta E, \Delta X_P, \Delta\delta_M; \mu, \omega) \tag{18}$$

The tooth surface containing design variables is referred to as the actual tooth surface, while the tooth surface obtained in the previous section is the theoretical tooth surface. When the machining adjustment parameters are modified, the spatial position of the actual tooth surface shifts, causing the center of the actual tooth surface to no longer coincide with that of the theoretical tooth surface. To align them, the actual tooth surface must be rotated by an angle θ until its midpoint coincides with that of the theoretical tooth surface. For an accurate evaluation of tooth surface form deviation, the

actual tooth surface needs to be rotated around the pinion rotation axis (X-axis) by a certain angle θ. The matrix representing this rotational transformation is expressed as:

$$M_X = \begin{bmatrix} 1 & 0 & 0 & 0 \\ 0 & \cos\theta & \sin\theta & 0 \\ 0 & -\sin\theta & \cos\theta & 0 \\ 0 & 0 & 0 & 1 \end{bmatrix} \tag{19}$$

All discrete points on the actual tooth surface can be calculated using the following formula:

$$\boldsymbol{r}_2 = M_X \boldsymbol{r}_1 \tag{20}$$

For any point A_{ij} (i=1,2,…,9; j=1,2,…,5) on the actual tooth surface, there exists a corresponding point P_{ij} on the theoretical tooth surface. The tooth surface deviation is defined as the projection of the vector difference between these two points onto the normal direction at point A_{ij} on the actual tooth surface. Thus, the expression for tooth surface deviation is given by:

$$\delta(\boldsymbol{x}) = \boldsymbol{r}_e(\boldsymbol{x};\omega,\mu) \cdot \boldsymbol{n}(\boldsymbol{x};\omega,\mu) \tag{21}$$

Here, x is a vector composed of the design variables, and:

$$\boldsymbol{r}_e = \boldsymbol{r}_2 - \boldsymbol{r}_1 \tag{22}$$

When all six design variables are introduced into the tooth surface deviation algorithm, the results are as shown in Figure 5. Due to the coupling effect of multiple parameters, significant deviations occur on the tooth surface, with a maximum error value of 69.7224 μm.

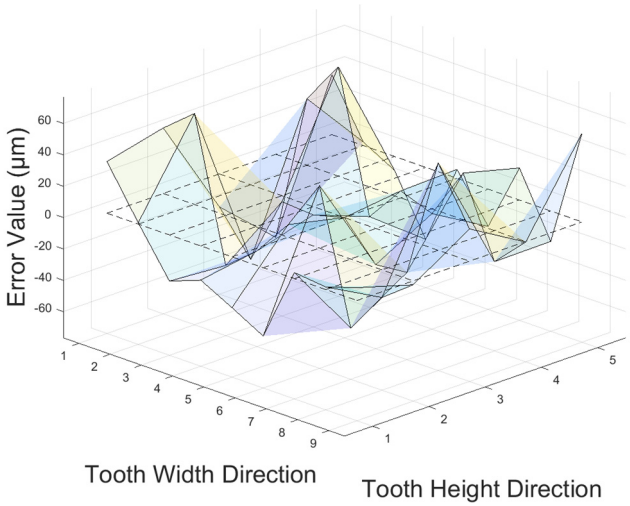

Figure 5. Influence of Multi-Parameter Coupling on Tooth Surface Deviation

For the P_{ij}-th point on the tooth surface, its position vector on the theoretical tooth surface is $\boldsymbol{r}_1^{(ij)}$, and its normal vector is $\boldsymbol{n}_{ij}$. The corresponding point on the actual tooth surface, calculated from the current machining adjustment parameters $\boldsymbol{x}_{ij}=[q_{ij}, S_{ij}, E_{ij}, X_{Bij}, X_{Pij}, \delta_{mij}]$,. The normal tooth profile deviation at this point is then defined as:

$$\delta_{ij}(\boldsymbol{x}) = (\boldsymbol{r}_2^{(ij)} - \boldsymbol{r}_1^{(ij)}) \cdot \boldsymbol{n}_{ij} \tag{23}$$

All discrete point deviations are constructed into an $i \times j$-dimensional deviation vector F($\boldsymbol{x}$):

$$F(x) = [\delta_{11}(\boldsymbol{x}), \delta_{12}(\boldsymbol{x}), ..., \delta_{ij}(\boldsymbol{x})]^T \tag{24}$$

The optimization objective is to seek an optimal set of design variables x^* that minimizes the sum of squares of the normal deviations at all discrete points. Accordingly, the following nonlinear least squares objective function is formulated:

$$\Phi(x) = \frac{1}{2} F(x)^T F(x) = \frac{1}{2} \sum_{i=1, j=1}^{i \times j} [\delta_{ij}(x)]^2 \tag{25}$$

This function directly and clearly reflects the degree of approximation between the actual tooth surface and the theoretical tooth surface in terms of tooth profile.

To achieve efficient numerical optimization, it is necessary to establish a quantitative relationship between changes in machine adjustment parameters and deviations, i.e., to solve for the gradient information of the objective function. The sensitivity matrix (Jacobian matrix) is defined as:

$$J_{kp}(x) = \frac{\partial \delta_k(x)}{\partial x_j}, k = 1, ..., 45; p = 1, ..., P \tag{26}$$

In the equation, J_{kp} represents the rate of change in the normal deviation δ_k at the k-th control point when the p-th machine parameter x_j undergoes a slight variation.

Given the complexity of the tooth surface equation, analytical solution of its partial derivatives is difficult. This paper adopts the forward difference method for numerical approximation, which provides sufficient accuracy and is easy to implement:

$$J_{kp}(x) \approx \frac{\delta_k(x + \Delta x_p e_p) - \delta_k(x)}{\Delta x_p} \tag{27}$$

Here, e_p is the p-th unit basis vector, and Δx_p is a small perturbation step size selected based on the physical meaning of the parameter.

3.2. Levenberg-Marquardt Optimization Algorithm

The problem defined by Equation (25) is a standard nonlinear least squares problem. The Levenberg-Marquardt (L-M) algorithm is widely employed for solving such problems due to its ability to effectively combine the advantages of the steepest descent method and the Gauss-Newton method, as well as its use of a damping factor to address ill-conditioned Jacobian matrices. This paper proposes a parameter optimization algorithm based on the L-M method.

In each iteration, the L-M algorithm obtains the parameter correction vector Δx by solving the following system of linear equations:

$$[J(x_i)^T J(x_i) + \lambda_i \boldsymbol{I}] \Delta x = -J(x_i)^T F(x_i) \tag{28}$$

where λ_i is the damping factor and $\boldsymbol{I}$ is the identity matrix. The adaptive adjustment strategy for the damping factor is the core of the L-M algorithm: when the iteration progresses well (i.e., Φ decreases rapidly), λ_i is reduced, causing the algorithm to approximate the Gauss-Newton method to accelerate convergence; when the iteration progresses poorly, λ_i is increased, causing the algorithm to approximate the steepest descent method to ensure stability. Consequently, the introduction of the damping coefficient enhances the stability and speed of the objective function's convergence.

The optimization solution process using the L-M algorithm is as follows:

1. Initialization:

Input the discrete point information of the target tooth surface $\{\boldsymbol{r}_1, \boldsymbol{n}_1\}$, i.e., the grid coordinates of the discrete points and their normal vectors. Set the initial machining parameters $x_0 = \{ q_0, S_0, E_0, X_{B0},$

X_{P0}, $\delta_{m0}\}$, convergence tolerance ε, maximum iteration count N_{max}, and initialize iteration counter i = 0.

2. Iteration Loop:

Tooth Surface Calculation and Deviation Evaluation: Based on the current parameters x_i, calculate the actual machined tooth surface using the generating motion model. Extract the discrete point coordinates $\boldsymbol{r}_2$ (x_i) corresponding to the theoretical tooth surface. Compute the normal deviation δ_k for all discrete points according to Equation (23), and construct the deviation vector $\boldsymbol{F}(x_i)$ and its norm $\| \boldsymbol{F}(x_i) \|$.

Convergence Check: If $\| \boldsymbol{F}(x_i) \| < \varepsilon$ or $i > N_{max}$, terminate the iteration and output the current parameter values $x^* = x_i$.

Sensitivity Matrix Calculation: Use the finite difference method to compute the Jacobian matrix $J(x_i)$ at the current parameter point. Each partial derivative component $\partial\delta_{ij}/\partial x_p$ reflects the sensitivity of the p-th machining parameter to the deviation at a specific point on the tooth surface.

Correction Vector Solution: Construct and solve the linear system of equations (28) according to the L-M equation to obtain the parameter increment (correction vector) Δx.

Tentative Update and Damping Factor Adjustment:Compute the tentative parameter vector: x_{test}= $x_i+\Delta x$. Calculate the objective function value at the tentative point: $\Phi(\boldsymbol{x}_{test})$. Compute the ratio of actual reduction to predicted reduction:

$$\rho = \frac{\Phi(\boldsymbol{x}_i) - \Phi(\boldsymbol{x}_i)}{\Delta \boldsymbol{x}\left(\lambda_i \Delta \boldsymbol{x} - \boldsymbol{J}(\boldsymbol{x}_i) T \boldsymbol{F}(\boldsymbol{x}_i)\right)} \tag{29}$$

If ρ>0.75, the approximation is favorable: accept the update (x_{i+1}= x_{test}), reduce the damping factor (λ_{i+1}=0.5λ_i), and steer the algorithm closer to the Gauss-Newton method to accelerate convergence.

If ρ<0.25, the approximation is poor: reject the update (x_{i+1}= x_i), increase the damping factor (λ_{i+1}=2λ_i), and steer the algorithm closer to the steepest descent method to enhance stability.

If 0.25≤ ρ≤ 0.75, accept the update and keep the damping factor unchanged (λ_{i+1}=λ_i).

Iteration Increment: Set i = i + 1 and return to step (1) to continue the iteration.

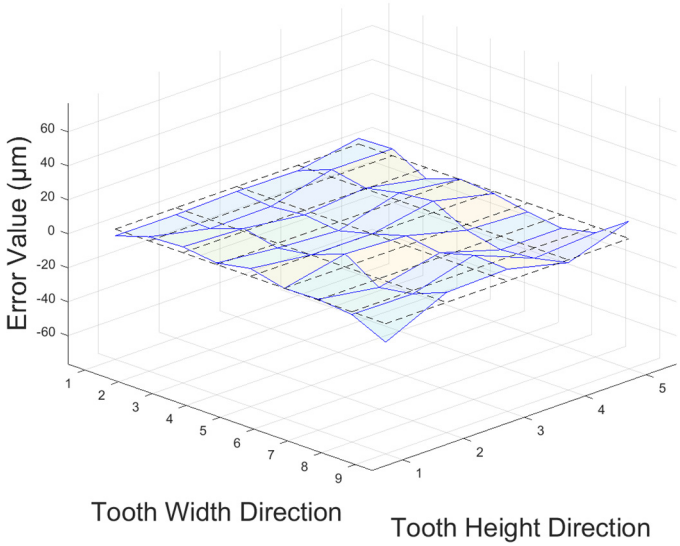

Figure 6. Optimization Results

After the iteration ends, output the optimal machining parameter combination x^*. Substitute this set of parameters into the tooth surface deviation calculation model for verification. The optimized tooth surface deviation distribution result, shown in Figure 6, demonstrates a significant reduction in the maximum deviation value to 8.26 μm, with very small error values at all discrete points. This verifies the effectiveness of the optimization algorithm and completes the optimization of the milling parameters.

4. CONCLUSION

(1) Based on the milling principle of spiral bevel gears, the structure of the spiral bevel gear milling machine and the motion relationships among its axes were analyzed, and a generating machining motion model for spiral bevel gears was established. By integrating the parameters of the milling cutter head with the generating machining motion model, a tooth surface model enveloped by the cutter head was developed.

(2) An analysis was conducted on the influence of six milling process parameters—such as angular tool position, radial tool position, and workpiece blank installation angle—on tooth surface deviation. Building on this foundation, an optimization model aimed at minimizing tooth surface deviation was constructed. The L-M algorithm was then employed to iteratively optimize the machining parameters with the goal of reducing the theoretical machining error as much as possible.

REFERENCES

[1] ZENG Tao. Design and Manufacturing of Spiral Bevel Gears [M]. Harbin: Harbin Institute of Technology Press, 1989: 91.

[2] LI Q M. Research on Tooth Surface Error Measurement and Correction Method for Hypoid Gears [D]. Wuhan University of Technology, 2020.

[3] SU J Z, HE C X. High-precision modification method for tooth surface of spiral bevel gears [J]. Journal of South China University of Technology (Natural Science Edition), 2014, 42(04): 91-96+104.

[4] CAI X W, FANG Z D. Algorithm research on reverse solving of machine tool settings for spiral bevel gears [J]. Journal of Mechanical Transmission, 2015, 39(03): 5-8+14.

[5] WANG X C, WANG J, JIANG H, LI R F, FENG W J. Tooth surface measurement and correction of machine settings for spiral bevel gears [J]. Journal of Mechanical Engineering, 2003, (08): 125-128.

[6] CHEN S H, YAN H Z. Research on tooth surface error correction algorithm for spiral bevel gears based with tilt method [J]. China Mechanical Engineering, 2011, 22(09): 1080-1084.

[7] NIE S W, DENG J, DENG X Z, YANG J J, LI J B. Equivalent correction method for tooth surface deviation of spiral bevel gears based on tooth surface Ease-off topology [J]. China Mechanical Engineering, 2017, 28(20): 2434-2440.

[8] Lin C Y , Tsay C B , Fong Z H . Computer-aided manufacturing of spiral bevel and hypoid gears with minimum surface-deviation[J]. Mechanism & Machine Theory, 1998, 33(6):785-803

[9] TANG J Y, NIE J A, WANG Z Q. Reverse correction method for spiral bevel gears machined by HFT method [J]. Journal of Central South University (Science and Technology), 2012, 43(06): 2142-2149.

[10] YAN Deshuang. Research on Forming Theory and Machining Method of Line Contact Tapered Spiral Bevel Gears [D]. Tianjin University, 2021.